

## 3D printed bio-models for medical applications

Yap, Yee Ling; Tan, Edgar Yong Sheng; Tan, Joel Heang Kuan; Peh, Zhen Kai; Low, Xue Yi;  
Yeong, Wai Yee; Tan, Colin Siang Hui; Laude, Augustinus

2017

Yap, Y. L., Tan, E. Y. S., Tan, J. H. K., Peh, Z. K., Low, X. Y., Yeong, W. Y., . . . Laude, A. (2017).  
3D printed bio-models for medical applications. *Rapid Prototyping Journal*, 23(2), 227-235.  
doi:10.1108/rpj-08-2015-0102

<https://hdl.handle.net/10356/143121>

<https://doi.org/10.1108/RPJ-08-2015-0102>

---

© 2017 Emerald Publishing Limited. All rights reserved. This paper was published in *Rapid Prototyping Journal* and is made available with permission of Emerald Publishing Limited.

*Downloaded on 26 Aug 2022 20:17:47 SGT*

# 3D Printed Bio-models for Medical Applications

---

*Yee Ling Yap, Yong Sheng Edgar Tan, Heang Kuan Joel Tan, Zhen Kai Peh, Xue Yi Low and Wai Yee Yeong*

Singapore Centre for 3D Printing, School of Mechanical and Aerospace Engineering, Nanyang Technological University, Singapore

*Colin Siang Hui Tan*

National Healthcare Group Eye Institute, Tan Tock Seng Hospital, Singapore, and

*Augustinus Laude*

National Healthcare Group Eye Institute, Tan Tock Seng Hospital, Singapore and School of Materials Science and Engineering, Nanyang Technological University, Singapore

## Abstract

**Purpose-** The design process of a bio-model involves multiple factors including data acquisition technique, material requirement, resolution of the printing technique, cost-effectiveness of the printing process and end-use requirements. This paper aims to compare and highlight the effects of these design factors to the printing outcome of bio-models.

**Design/Approach-** Different data sources including engineering drawing, computerised tomography (CT), and Optical Coherence Tomography (OCT), were converted to printable data format. Three different bio-models: an ophthalmic model, a retina model and a distal tibia model were printed using 2 different techniques, namely PolyJet and Fused Deposition Modelling. The process flow and 3D printed models were analysed.

**Finding-** The data acquisition and 3D printing process affect the overall printing resolution. The design process flows utilizing different data sources were established and the bio-models were printed successfully.

**Research Limitation-** The data acquisition techniques contained inherent noise data and resulted in inaccuracies during data conversion.

**Originality-** Our work demonstrated that the data acquisition and conversion technique carried significant effect to the quality of the bio-model blueprint and subsequently the printing outcome. In addition, important design factors of bio-models were highlighted such as material requirement and the cost-effectiveness of the printing technique. This paper provides a systematic discussion for future development of an engineering design process in 3D printed bio-models.

**Keywords** Rapid prototyping, 3D printing, Additive manufacturing, Bio-model, Data acquisition, Data conversion

## Introduction

Bio-model is an entity that replicates the geometry or form of a biological structure. These models can be realized in either virtual or physical forms. In recent years, Additive Manufacturing (AM) principles have been adopted to produce three-dimensional (3D) customised physical implants (Yeong et al., 2004, Chua et al., 2005) and anatomical models (Chua and Leong, 2014).

Conventional methods of replicating bio-models from actual anatomies includes the use of virtual model on the computer, or creating a physical one through casting method of selected polymers (Massimiliano et al., 2008). Study has shown that recognition performance was significantly better for real objects as compared to a virtual image and thus analysing the processes and parts using the virtual model is considered to be more challenging and less effective (Snow et al., 2014). A casted polymer model also takes a longer time to fabricate and incur a higher cost of customisation.

AM technology has enabled the fabrication of patient-specific, intricate and accurate models without the need of skilled artists or sculptors. As a result, medical teams were able to reduce time and resources to acquire a 3D physical model. Such bio-models have been particularly useful in providing surgeons accurately defined human anatomic structures and disorders, which are highly complex and difficult to be analysed using virtual model.

Generally, as illustrated in Figure 1, there are four main medical applications of 3D printed bio-models, specifically:

### A) Preoperative Planning and Practicing

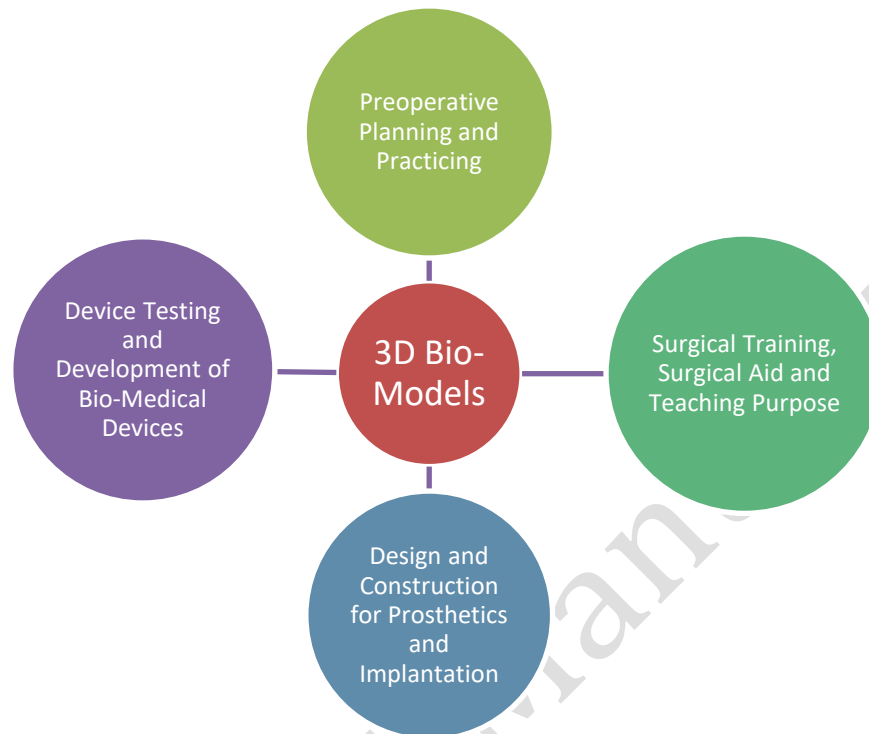
One important use of bio-models is as aiding tools for surgical planning and rehearsal. They have played a significant role by providing a visual and physical replica of the actual part, enabling surgeons to familiarise prior to the operation (Yusoff et al., 2012). Custom-made parts produced by 3D printing methods, had been used for simulation purposes in operations involving craniomaxillofacial reconstruction (Aung et al., 1999, Yusoff et al., 2012), the spine (Izatt et al., 2007), and cerebral aneurysm (Wurm et al., 2004), with great accuracies. The development of multiple materials 3D printing has also allowed the fabrication of models such as liver (Noecker et al., 2006) and heart (Zein et al., 2013) to be analysed by surgeons more accurately using coloured and flexible materials. .

### B) Surgical Training, Surgical Aid and Teaching Purpose

3D printed models can be used as teaching and training aids for young surgeons and researchers. The models are made in colours to provide a better illustration of anatomy, allow viewing of internal structures and better understanding of problems (Waran et al., 2014, Shiraishi et al., 2010). The emergence of new and rapidly growing treatment methods, for example cardiovascular surgery requires greater training opportunities and a precise identification of the heart structures and its disease for surgeons (Abdel-Sayed and von Segesser, 2011). A neuroanatomical study also shows that 3D physical modelling activity was proven to improve the effectiveness for teaching spatial relationships of brain anatomy

and the students performed significantly better on the understanding of periventricular structures (Estevez et al., 2010).

**Figure 1** Four main applications of 3D printed bio-models



### C) Design and Construction for Prosthetics and Implantation

3D printing techniques are time and cost efficient in making customised prostheses and implants as it is able to quickly fit prosthesis to a patient using Computerised Tomography (CT) scan. 3D printing techniques were used to fabricate hip sockets, spinal implants and knee joints (Ballyns et al., 2008). D'Urso et al. (1998) used models reproduced by Stereolithography (SLA) method in craniofacial surgery for patients who suffered complex craniofacial abnormalities, where standard imaging failed to clearly differentiate the anatomical pathology. Biocompatible facial prostheses that were lightweight and possessed realistic skin colour were generated using Z-Corp 3D printer (Zardawi, 2013). In recent years, 3D printed metallic implants, especially for orthopaedic (Sing et al., 2015) and craniomaxillofacial (Jardini et al., 2014) applications, are on the rise as they provide faster and more flexible manufacturing routes compared to conventional manufacturing methods. Indirect 3D printing were also developed to shape non-printable materials into complex shape (Yeong et al., 2005).

## D) Device Testing and Development of Bio-Medical Devices

Physical bio-models were used for load testing where in-vivo measurements are impossible or unfeasible. Thereafter, results were reviewed against computational bio-models. For example, loads and moments on the oral implant and the denture bearing area of a mandible SLA model was obtained using strain gauges. The model was found to be reliable with an error of 10–20% (Heckmann et al., 2001). In addition, in the search for realistic phantoms for vascular studies, PolyJet was successfully utilised for constructing more realistic compliant parts like the aortic model (Biglino et al., 2013) and vascular model (Markl et al., 2005) for in-vitro studies and device testing.

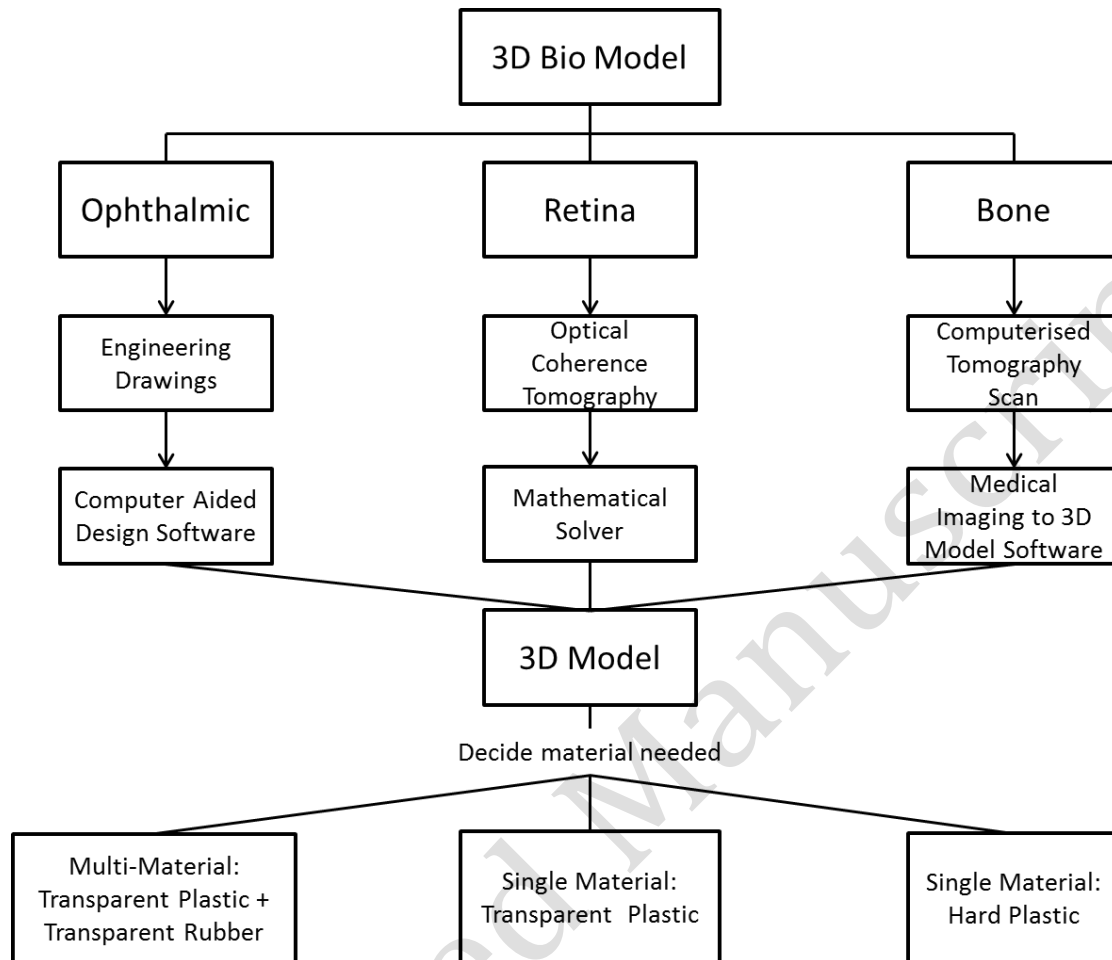
For creating 3D models, data is obtained either by hand drawing or scanning of actual objects. Next the data is processed by computer software depending on the data source. The models can be drawn in the computer using Computer Aided Design (CAD) software while software dedicated to converting the CT medical imaging data in DICOM to STL (STereoLithography), which is readable by all 3D printing machines, is used. Once the 3D model is ready, the materials required are to be selected based on the application and the purpose of each bio-models. Base on the materials required, the type of 3D printing techniques and thus the 3D printers can be chosen.

Generally, the design process of a bio-model involves multiple factors including data acquisition technique, material requirement, printing resolution, cost-effectiveness of the printing process and end-use requirements. This paper aims to compare and highlight the effects of these design factors on the printing outcome of a bio-model. Three different data acquisition and conversion techniques were demonstrated and discussed. Three bio-models: ophthalmic, retina and distal tibia models were printed using 2 techniques, namely PolyJet and Fused Deposition Modelling (FDM).

### Methods

In this study, ophthalmic, retina and distal tibia models were developed to illustrate the versatility of 3D printing. In each of the cases, different AM processes, material and data acquisition techniques were used, before deriving the 3D printed bio-model, as shown in Figure 2. The ophthalmic model requires multiple materials with different tactile properties to highlight different tissues in the ophthalmic model, limiting the printing technique selection to PolyJet 3D printer that can print both hard and rubbery plastics simultaneously. As the retina model is mainly used for patient education, the part should be produced with the least cost and time. PolyJet printing technique was thus selected as for high resolution and high speed printing, as compared to other techniques. The distal tibia model, which is used for preoperative planning, requires accurate and robust physical representation. Hence, FDM that uses hard plastic material can be utilised in the fabrication of the bone model.

**Figure 2** Design and fabrication process flows of 3D printed bio-models



### Ophthalmic model for surgical training

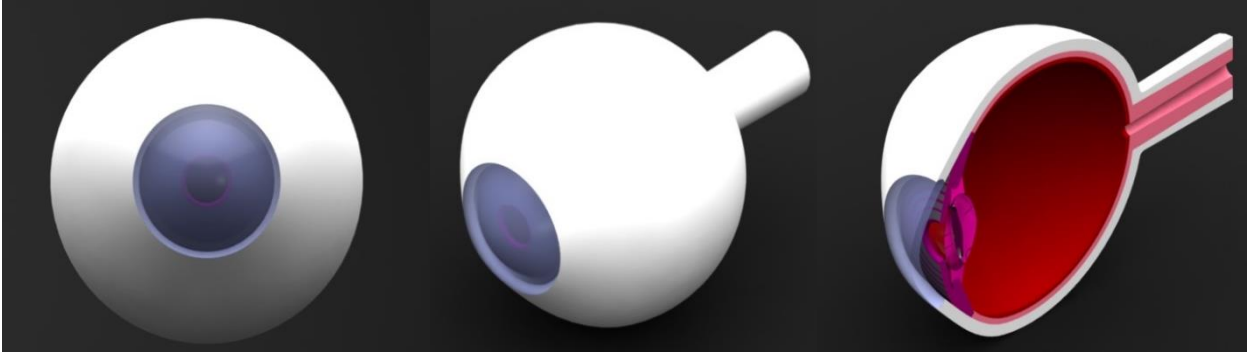
To fabricate an ophthalmic model, several factors including colour, texture and elasticity of the material has to be made similar to the organ of interest. A framework to position each part of the organ was worked out using multiple illustrations found in medical books to determine the exact dimensions of the eye (Hashemi et al., 2015). The model was mapped and illustrated using CAD package, Solidworks, as shown in Figure 3(a)-3(c). The model was separated into parts depending on the tissues and their features.

As the shape of the ophthalmic model approaches a hollow spherical ball, there will be support materials filled in the cavity to support the building of the upper hemisphere part. In order to enable removing of the support materials and the injection of gel into the coat in post-processing stage, the eye model is further modified into two designs: Design 1 and Design 2, with different assembling methods as shown in Figure 3(d) and Figure 3(e), respectively.

The ophthalmic model was fabricated using Objet500 Connex3 (3D printer, Stratasys, Ltd.), one of the established multi-material polymer 3D printing technique (Khoo et al., 2015). It creates parts by jetting very thin layers (approximate 16 -32  $\mu\text{m}$ ) of liquid photopolymer onto a build tray, layer by layer. Model and support materials will be deposited selectively and they are cured instantly with UV light after they are jetted, Support materials can be removed by water jetting during the post-processing. The combination of rubber-like and rigid ABS-like materials provides broader range of materials with varying physical properties, allowing the construction of ophthalmic models with similar properties to the human eye.

Table I shows the physical properties of different ophthalmic components. Different combination of polymer were selected according to their hardness and Young's modulus to simulate similar texture and tactility of the eye. PolyJet digital materials made up of TangoPlus, VeroClear and VeroWhite closely resemble most of the parts, except for iris, zonular fibre and ciliary muscles, as shown in Table I. Digital materials with the closest property were hence used for these parts. Gelatin was used to simulate the gel-like vitreous humour and it was injected into the chamber via the hole in the optic nerve path. 3D printed ophthalmic models of Designs 1 and 2 after assembly and gel injection are shown in Figure 4(a) and 4(b), respectively.

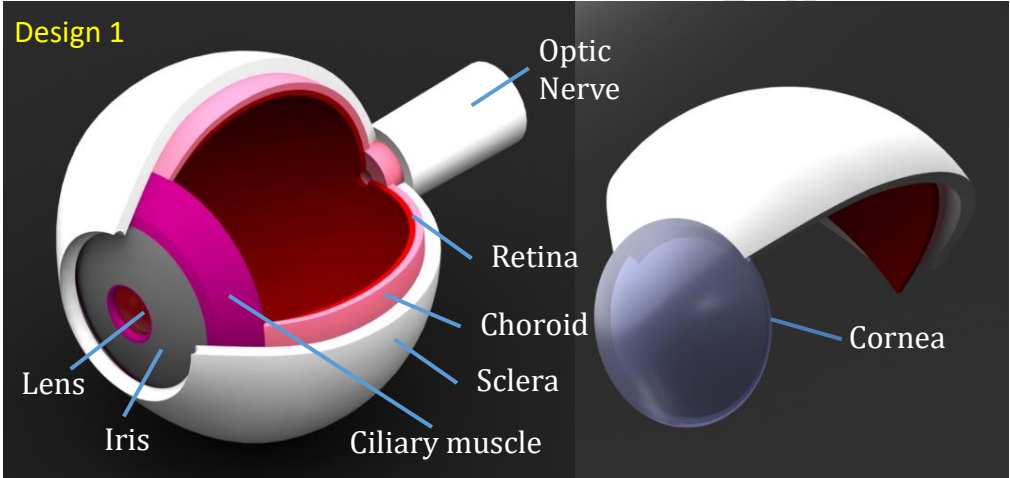
**Figure 3** Final render of a complete ophthalmic model (a) front view, (b) isometric view, (c) sectional view, (d) Design 1: (left)  $\frac{3}{4}$  of the ophthalmic model without cornea, (right) cornea and  $\frac{1}{4}$  of ophthalmic coats, (e) Design 2: (left) cornea, (middle)  $\frac{2}{3}$  of ophthalmic model, (right)  $\frac{1}{3}$  of the sclerotic chamber with optic nerve



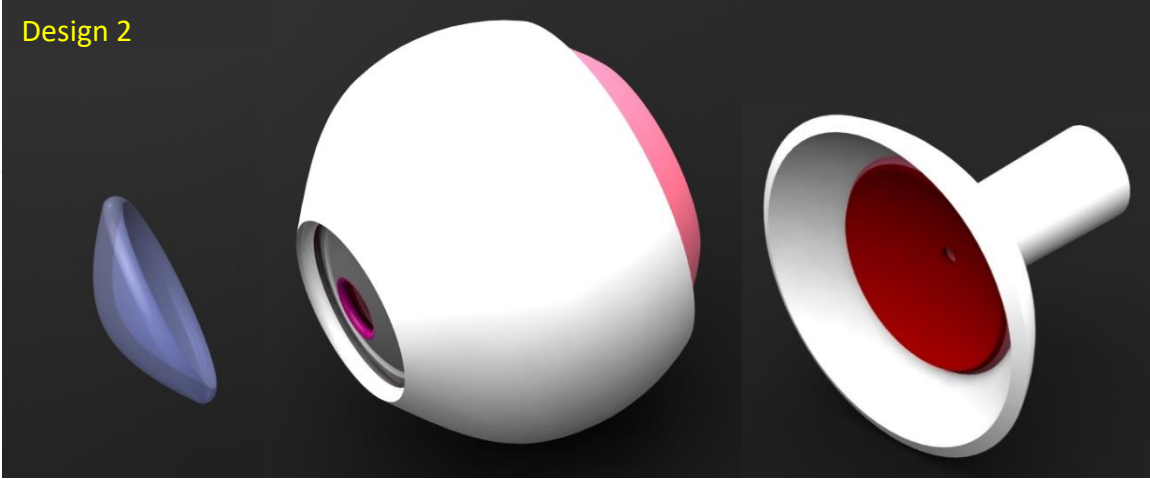
(a)

(b)

(c)



(d)



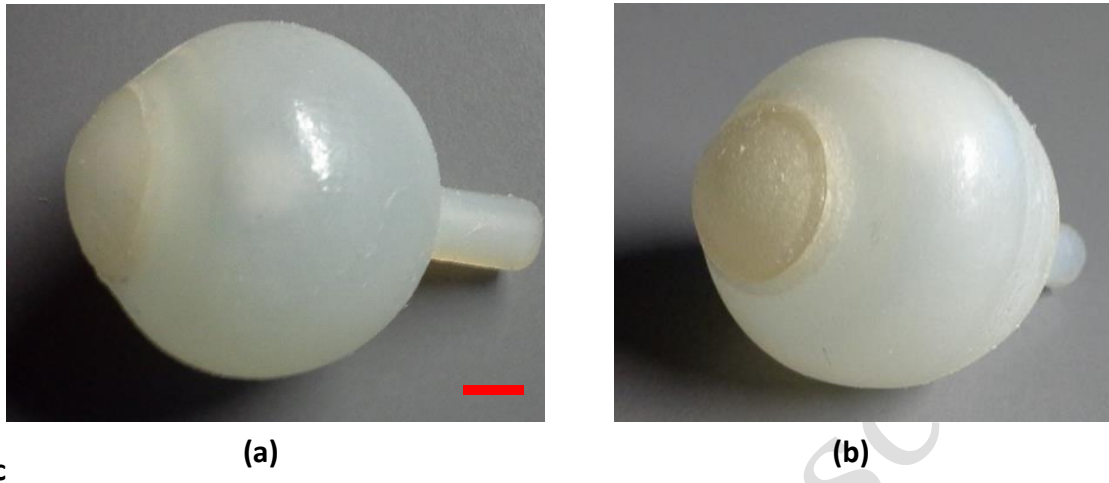
(e)



**Table I** Physical properties of ophthalmic components and the digital materials selected for each components for PolyJet printing

<b>Parts</b>	<b>Young Modulus (kPa)</b>	<b>Thickness (mm)</b>	<b>Characteristic</b>	<b>References</b>	<b>Digital Materials</b>
<b>Sclera</b>	$1.8 \times 10^3 - 2.9 \times 10^3$	0.43 – 1.10	White and flexible	(Friberg and Lace, 1988, Olsen et al., 1998)	FLX9985
<b>Choroid</b>	$2.2 \times 10^2 - 7.5 \times 10^2$	0.20 – 0.47	Flexible	(Friberg and Lace, 1988, Ikuno et al., 2010)	FLX9770
<b>Retina</b>	20 - 24.5 [53]	0.17 – 0.40	Flexible	(Hashemi et al., 2015, Asrani et al., 1999)	FLX9740
<b>Lens</b>	$0.5 \times 10^3 - 1.5 \times 10^3$	central thickness $\approx$ 3.60	Transparent and flexible	(Ziebarth et al., 2011, van Alphen and Graebel, 1991)	FLX9970
<b>Cornea</b>	$1.0 \times 10^2 - 1.0 \times 10^4$	central thickness $\approx$ 0.50 – 0.60	Transparent and flexible	(Elsheikh et al., 2007, Ventura et al., 2001)	FLX9970
<b>Ciliary muscle</b>	$1.20 \times 10^2$	-	Flexible	(van Alphen and Graebel, 1991)	FLX9750
<b>Zonular Fibre</b>	$3.50 \times 10^2$	-	Flexible	(van Alphen and Graebel, 1991)	FLX9760
<b>Pupil</b>	-	-	Flexible	-	-
<b>Iris</b>	9.0	-	Flexible	(Heys and Barocas, 2002)	FLX930
<b>Aqueous humour</b>	Density = $1000\text{kg/m}^3$	-	Clear fluid	(Fitt and Gonzalez, 2006)	-
<b>Vitreous humour</b>	Density = $1000\text{kg/m}^3$	-	Liquid/clear gel	(Shelby, 2004)	-

**Figure 4** 3D printed ophthalmic model after assembly and gel injection: (a) Design 1, (b) Design 2 (Scale: 5mm)



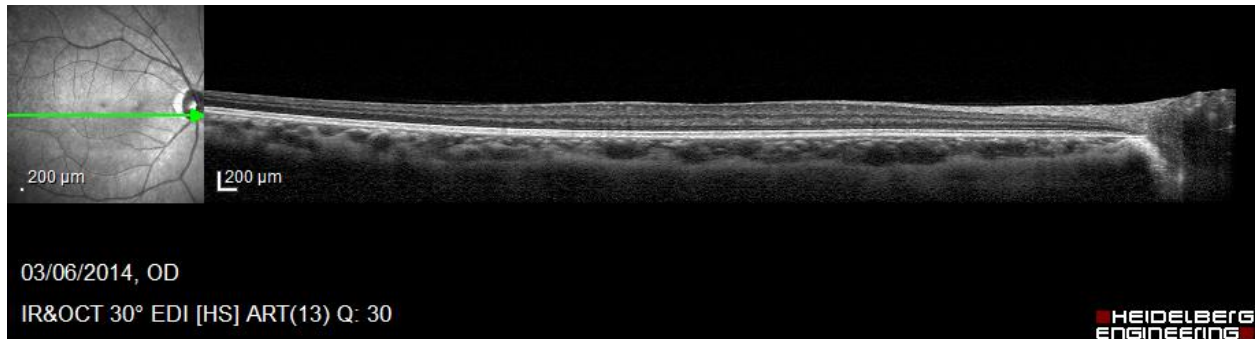
### Retina model for patient education

The prevalence of age related macular degeneration has been rising in recent years. These diseases increase the risk of the patient losing their sense of sight. As such, 3D physical eye models may give the patients better understanding of the diseases. Optical Coherence Tomography (OCT) was taken from an eye to test the feasibility to use such technology to convert these data to a printable format.

An OCT scan was performed using Heidelberg Spectralis (Heidelberg Engineering, Heidelberg, Germany) covering 30 degrees of the retina, as shown in Figure 5(a). This provided high resolution image of the retina with micrometre resolution using non-invasive, light scattering technique. The data was converted using MATLAB (MathWorks, Natick, Massachusetts, USA). Based on the scale given in the OCT images, data points were rescaled to accurately reflect the exact size. The slices were then cropped to remove redundant data and the image was segmented. The final slice products were merged and a voxel data was produced from 3D data points. This data enabled the conversion of the image to the STL format. Finally, noise shells were removed from the STL files using Magics (Materialise, Leuven, Belgium), resulting in a single uniform shell.

Since the objective of the model is to educate the patient on the disease, the model was scaled up by 20 times for 3D printing. The retina bio-model was fabricated by PolyJet Eden350V using transparent material (RGD720). PolyJet 3D printing process was chosen to produce the intricate details and many small undulations at fine resolution. The completed retina model is shown in Figure 5(b) and 5(c).

**Figure 5** (a) An OCT image of the retina layer, (b) a PolyJet printed enlarged retina layer in frontal view, (c) side view of the printed retina model (Scale: 5mm)



(a)



(b)

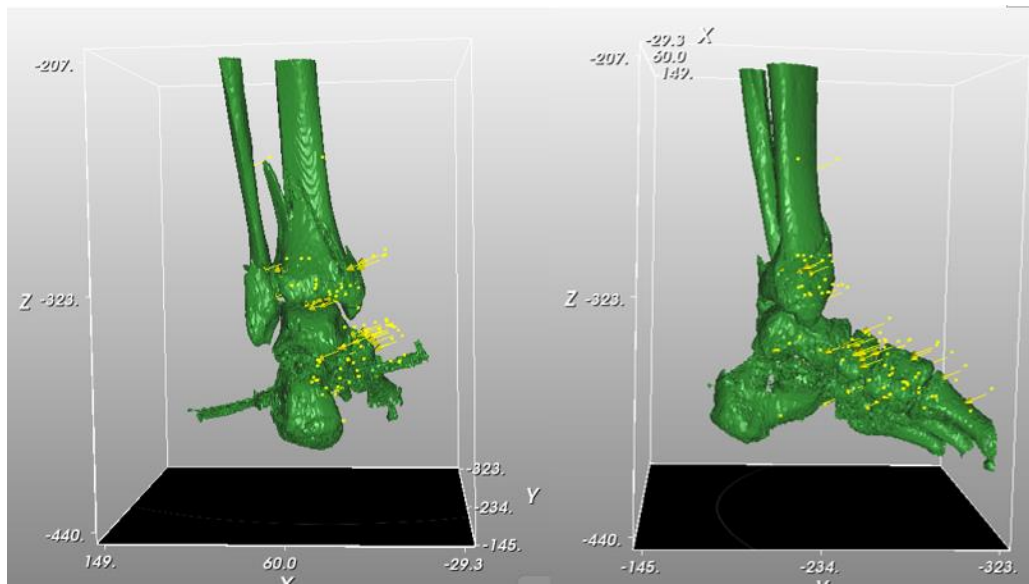


(c)

### Distal tibia for preoperative planning

CT scan was utilised to acquire accurate images of the fragmented bone. CT scan creates images of patient by combining multiple data of X-ray images to produce a slice copy of an area of interest. The acquired data, which relates to the density of the material, can be used to determine the position of bones and bone fragment in the body. In this example the CT scan data was obtained in DICOM format with 292 scan slices. These images were merged and the mesh surface was extracted into STL format using the software DeVIDE (v9. 8.3784). The model was fabricated using Stratasys Dimension Elite, a FDM 3D printer with ABSplus model. The printed model was submerged into sodium hydroxide solution to dissolve the support material. The accuracy and resolution of the FDM model which is about 0.1mm is sufficient to assist surgeons in diagnosis and pre-operative planning. In addition, this technique is relatively quick for reconstructing physical bio-models.

**Figure 6** Distal tibia model: (a) back view and side view of virtual distal tibia model, (b) FDM distal tibia model in front view and back view (Scale: 20mm)



(a)



(b)

## Result Analysis

The completed model as shown in Figure 6(b) was measured to compare its dimensions with the virtual model. The physical model was measured using vernier caliper while the 3D virtual model was measured via software Meshmixer. The measurement result as presented in Table II shows that the 3D printed model only has up to 2% deviation from the virtual model. The physical models are easy and intuitive to work with as the surgeons can physically plan the best operative procedures and personalized-fit treatment using the patient-specific model to reduce the operating time and avoid re-operation on the patient.

**Table II** Dimensional accuracy of FDM distal tibia model compare to the virtual distal tibia model

Distal Tibia Measurement	Physical model (mm)	Virtual model (mm)	Accuracy
Height	147.19	146.94	0.17%
Width (Upper part)	49.97	49.195	1.58%
Width (Lower part)	66.12	66.246	-1.90%
		Average	1.21%

## Discussion and Results

### Design Considerations

Depending on the application of 3D printed bio-model, the required dimensional tolerance of the printed model will vary. The expected tolerances of the bio-models for different applications are shown in Figure 7. Applications that are built towards patient's education do not need to be as stringent as those that are used for device testing or those that are built for prosthetics uses. The tolerance of the 3D printed model is dependent on the resolution of the 3D printer.

The differences in resolution requirement accommodate the shortcomings derived from data acquisition and printing resolution. The successful generation of an accurate 3D printed anatomic model is thus largely attributed to two aspects - the quality of medical data acquisition technique and the manufacturing performance of 3D printing. Clinical data acquisition is typically achieved at high spatial resolution of 400-600  $\mu\text{m}$  with high contrast through the use of various imaging modalities, for examples magnetic resonance imaging (MRI), ultrasonography, CT and OCT (Rengier et al., 2010).

### Acquisition Technique

Generally, the acquisition technique used is based on size, required resolution and the application of the bio-model. OCT uses light interferometry to record the depth and path length of the photons. OCT can achieve an accuracy of 1  $\mu\text{m}$  axial resolution by using laser of 800nm (Drexler et al., 2001). However, this method is only applicable for biological tissues that are 1-2mm below the surface. The typical axial resolution of current OCT devices ranges from 5 to 7  $\mu\text{m}$ . CT scan, on the other hand, uses X-Ray to penetrate through the body to acquire the 3D image. The resolution of the data collected from CT scan is about 100  $\mu\text{m}$ . The complexity of the eyes will not be able to be reflected through the use of such imaging technique. The ophthalmic model was thus modelled by CAD technique using literature knowledge. The 3 acquisition techniques were evaluated in Table III.

**Figure 7** Expected tolerance of the 3D printed bio-models for different applications

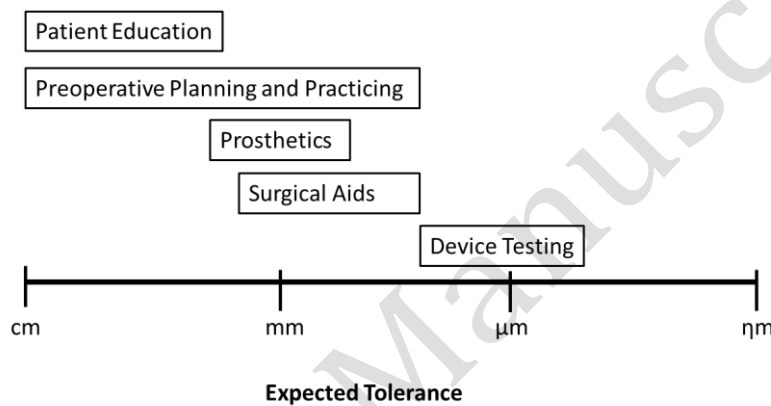


**Table III** Evaluation of data acquisition techniques

Acquisition Technique	Image Resolution	Conversion Compatibility	Application
<b>CAD Engineering Design</b>	N/A	Can be saved to STL directly from CAD	Any design for hard and soft tissue
<b>CT</b>	100 $\mu\text{m}$	Similar software as DeVIDE could be used to save as STL	Hard and soft tissues and bones
<b>OCT</b>	1-15 $\mu\text{m}$	Similar mathematical solvers as MATLAB could be used to convert the images to STL	Sub-surface scanning Suitable for ophthalmic tissue

**Data Conversion Method**

The data conversion techniques were chosen based on the data source. DICOM files from the CT scan can be easily converted to STL files due to the abundance of easy-to-use open source and paid programs. The resultant CT data can be easily converted to 3D objects by inputting the appropriate Hounsfield value for segmentation. OCT, on the other hand, has to be converted using basic coding via Matlab Programming. This is because the OCT output data is only an image data as compared to the CT data which is based on Hounsfield value. The program has to be written in house and exporting the STL files by representing each voxel with a solid. Image segmentation was based from individual data input and thus has a personal perspective on where the resulting retina is found.

### **3D Printing Technique**

**Materials.** The materials used in the fabrication of bio-models were determined by the 3D printing process, the resolution and the material similarity to the intended organ or tissue. The materials could be selected and tuned accordingly to fit the purpose or application (Yap and Yeong, 2014). With current multi-material printing technology, a wide range of materials from rigid to flexible and from transparent to coloured are available to fabricate the model in only one printing. The development of ophthalmic model consisting of multiple materials was attributed to the 3D printer's capability to formulate different composition in a single process. Various layers and components of an ophthalmic model can be duplicated for its tactile properties. This combination of materials with different tactile properties was not easily achievable by traditional technique of producing 3D bio-models. Fabrication of this multitude provides an enhanced feature that allows the model to have different material characteristics at different parts.

**Resolution achieved.** The fabrication of complex and detailed bio-models is limited by the 3D printing resolution. As shown in Table IV, PolyJet technique is capable of replicating fine features with greater than 16  $\mu\text{m}$  while FDM technique is limited to producing features that are above 250  $\mu\text{m}$ . It can be deduced that the achievable resolution can effectively serve as patient education, surgical aids, surgical planning and practicing, as well as prosthetics construction.

**Printing time and cost.** The printing time and cost of materials are critical factors in fabricating bio-models. The printing time of FDM distal tibia took about 15 hours and it is critical when emergency treatment is needed. The printing time of PolyJet process is relatively short, ranging from 30 minutes for retina model to 1.5 hours for ophthalmic model. The cost of FDM materials is approximately half of that of PolyJet materials. 3D printed bio-models could be customised according to the needs of medical teams and can be produced in a shorter time as compared to conventional 3D bio-models.

**Table IV** Evaluation of bio-models printing techniques

<b>Printing Technique</b>	<b>Resolution</b>	<b>Material</b>	<b>Advantages</b>	<b>Time</b>	<b>Cost</b>
<b>PolyJet</b>	16um (Yap et al., 2014, Yap and Yeong, 2015, Lee et al., 2016)	Various materials including transparent, rubbery and hard materials	Great Precision, able to print multi-materials in different colours and hardness	Fast	\$\$
<b>FDM</b>	>250um (Berger, 2015)	Robust materials such as ABS	Strong and robust plastics available	Slow	\$

## Conclusion

This paper provides a systematic discussion for future engineering design process of 3D printed bio-models. In this study, the ophthalmic model and retina model were successfully printed using PolyJet technology. The ophthalmic model was printed in different tactile properties and flexibility that mimic human tissue. It was reconstructed with similar shape and multiple tissues which present a more realistic bio-model in medical training environment. Hence, this application has the potential to aid in surgical simulation and create bio-models which may be used in medical device testing. Retina model was scaled up and printed to illustrate the details for patient education

Fabrication of distal tibia model was achieved using FDM after CT scan data processing. The technique of transferring 2D data images to a physical 3D printed bio-model is more effective in identifying the types for fracture for pre-operative planning.

3D printing is a promising technology in bio-models fabrication due to its capabilities to replicate human complex anatomy. They are useful in disease visualization, pre-operative planning, surgical simulation and medical education. With meticulous planning, different parts of human anatomy that fulfil the requirements are possible to be 3D printed in a short period with high accuracy. This paper has also demonstrated that multi-materials and multi-colour 3D printing have the potential to produce lifelike bio-models with true physical characteristics to enhance the study of human anatomy and analysis of diseases.

## Acknowledgement

This work was supported under NHG ARG grant 14009 and NTU start up grant.



## References

- Abdel-Sayed, P. & Von Segesser, L. K. (2011), *Rapid Prototyping for Training Purposes in Cardiovascular Surgery*, INTECH Open Access Publisher.
- Asrani, S., Zou, S., D'anna, S., Vitale, S. & Zeimer, R. (1999), "Noninvasive mapping of the normal retinal thickness at the posterior pole", *Ophthalmology*, Vol. 106 No. 2, pp. 269-273.
- Aung, S. C., Tan, B. K., Foo, C. L. & Lee, S. T. (1999), "Selective laser sintering: application of a rapid prototyping method in craniomaxillofacial reconstructive surgery", *Ann Acad Med Singapore*, Vol. 28 No. 5, pp. 739-43.
- Ballyns, J. J., Gleghorn, J. P., Niebrzydowski, V., Rawlinson, J. J., Potter, H. G., Maher, S. A., Wright, T. M. & Bonassar, L. J. (2008), "Image-guided tissue engineering of anatomically shaped implants via MRI and micro-CT using injection molding", *Tissue Engineering Part A*, Vol. 14 No. 7, pp. 1195-1202.
- Berger, U. (2015), "Aspects of accuracy and precision in the additive manufacturing of plastic gears", *Virtual and Physical Prototyping*, Vol. 10 No. 2, pp. 49-57.
- Biglino, G., Verschuere, P., Zegels, R., Taylor, A. M. & Schievano, S. (2013), "Rapid prototyping compliant arterial phantoms for in-vitro studies and device testing", *Journal of Cardiovascular Magnetic Resonance*, Vol. 15 No. 1.
- Chua, C. K. & Leong, K. F. (2014), *3D Printing and Additive Manufacturing: Principles and Applications* World Scientific Publishing Co Pte Ltd, Singapore.
- Chua, C. K., Yeong, W. Y. & Leong, K. F. (2005), "Rapid prototyping in tissue engineering: a state-of-the-art report", *Virtual Modeling and Rapid Manufacturing*, pp. 19-27.
- D'urso, P. S., Atkinson, R. L., Bruce, I. J., Effene, D. J., Lanigan, M. W., Earwaker, W. J., Holmes, A., Barker, T. M. & Thompson, R. G. (1998), "Stereolithographic (SL) biomodelling in craniofacial surgery", *British Journal of Plastic Surgery*, Vol. 51 No. 7, pp. 522-530.
- Drexler, W., Morgner, U., Ghanta, R. K., Kärtner, F. X., Schuman, J. S. & Fujimoto, J. G. (2001), "Ultrahigh-resolution ophthalmic optical coherence tomography", *Nature medicine*, Vol. 7 No. 4, pp. 502-507.
- Elsheikh, A., Wang, D. & Pye, D. (2007), "Determination of the modulus of elasticity of the human cornea", *Journal of refractive surgery (Thorofare, NJ: 1995)* No. 23, pp. 808-18.
- Estevez, M. E., Lindgren, K. A. & Bergethon, P. R. (2010), "A novel three-dimensional tool for teaching human neuroanatomy", *Anat Sci Educ*, Vol. 3 No. 6, pp. 309-17.
- Fitt, A. D. & Gonzalez, G. (2006), "Fluid mechanics of the human eye: aqueous humour flow in the anterior chamber", *Bulletin of mathematical biology*, Vol. 68 No. 1, pp. 53-71.
- Friberg, T. R. & Lace, J. W. (1988), "A comparison of the elastic properties of human choroid and sclera", *Experimental eye research*, Vol. 47 No. 3, pp. 429-436.
- Hashemi, H., Khabazkhoob, M., Emamian, M. H., Shariati, M., Yekta, A. & Fotouhi, A. (2015), "White-to-white corneal diameter distribution in an adult population", *Journal of Current Ophthalmology*, Vol. 27 No. 1-2, pp. 21-24.
- Heckmann, S. M., Wichmann, M. G., Winter, W., Meyer, M. & Weber, H. P. (2001), "Overdenture attachment selection and the loading of implant and denture - bearing area. Part 1: In vivo verification of stereolithographic model", *Clinical oral implants research*, Vol. 12 No. 6, pp. 617-623.
- Heys, J. J. & Barocas, V. H. (2002), "Computational evaluation of the role of accommodation in pigmentary glaucoma", *Investigative ophthalmology & visual science*, Vol. 43 No. 3, pp. 700-708.

- Ikuno, Y., Kawaguchi, K., Nouchi, T. & Yasuno, Y. (2010), "Choroidal thickness in healthy Japanese subjects", *Investigative ophthalmology & visual science*, Vol. 51 No. 4, pp. 2173-2176.
- Izatt, M. T., Thorpe, P. L., Thompson, R. G., D'urso, P. S., Adam, C. J., Earwaker, J. W., Labrom, R. D. & Askin, G. N. (2007), "The use of physical biomodelling in complex spinal surgery", *Eur Spine J*, Vol. 16 No. 9, pp. 1507-18.
- Jardini, A. L., Larosa, M. A., De Carvalho Zavaglia, C. A., Bernardes, L. F., Lambert, C. S., Kharmandayan, P., Calderoni, D. & Maciel Filho, R. (2014), "Customised titanium implant fabricated in additive manufacturing for craniomaxillofacial surgery", *Virtual and Physical Prototyping*, Vol. 9 No. 2, pp. 115-125.
- Khoo, Z. X., Teoh, J. E. M., Liu, Y., Chua, C. K., Yang, S., An, J., Leong, K. F. & Yeong, W. Y. (2015), "3D printing of smart materials: A review on recent progresses in 4D printing", *Virtual and Physical Prototyping*, Vol. 10 No. 3, pp. 103-122.
- Lee, J. M., Zhang, M. & Yeong, W. Y. (2016), "Characterization and evaluation of 3D printed microfluidic chip for cell processing", *Microfluidics and Nanofluidics*, Vol. 20 No. 1, pp. 1-15.
- Markl, M., Schumacher, R., Küffer, J., Bley, T. A. & Hennig, J. (2005), "Rapid vessel prototyping: Vascular modeling using 3t magnetic resonance angiography and rapid prototyping technology", *Magnetic Resonance Materials in Physics, Biology and Medicine*, Vol. 18 No. 6, pp. 288-292.
- Massimiliano, F., Francesca De, C., Franco, P., Stefano, B. & Giorgio, G. (2008), "3D restitution, restoration and prototyping of a medieval damaged skull", *Rapid Prototyping Journal*, Vol. 14 No. 5, pp. 318-324.
- Noecker, A. M., Chen, J.-F., Zhou, Q., White, R. D., Kopcak, M. W., Arruda, M. J. & Duncan, B. W. (2006), "Development of Patient-Specific Three-Dimensional Pediatric Cardiac Models", *ASAIO Journal*, Vol. 52 No. 3, pp. 349-353 10.1097/01.mat.0000217962.98619.ab.
- Olsen, T. W., Aaberg, S. Y., Geroski, D. H. & Edelhauser, H. F. (1998), "Human sclera: thickness and surface area", *American journal of ophthalmology*, Vol. 125 No. 2, pp. 237-241.
- Rengier, F., Mehndiratta, A., Von Tengg-Kobligh, H., Zechmann, C. M., Unterhinninghofen, R., Kauczor, H. U. & Giesel, F. L. (2010), "3D printing based on imaging data: review of medical applications", *International Journal of Computer Assisted Radiology and Surgery*, Vol. 5 No. 4, pp. 335-341.
- Shelby, J. E. (2004), "Density of vitreous silica", *Journal of non-crystalline solids*, Vol. 349, pp. 331-336.
- Shiraishi, I., Yamagishi, M., Hamaoka, K., Fukuzawa, M. & Yagihara, T. (2010), "Simulative operation on congenital heart disease using rubber-like urethane stereolithographic biomodels based on 3D datasets of multislice computed tomography", *European Journal of Cardio-Thoracic Surgery*, Vol. 37 No. 2, pp. 302-306.
- Sing, S. L., An, J., Yeong, W. Y. & Wiria, F. E. (2015), "Laser and electron-beam powder-bed additive manufacturing of metallic implants: A review on processes, materials and designs", *Journal of Orthopaedic Research*. DOI: 10.1002/jor.23075
- Snow, J. C., Skiba, R. M., Coleman, T. L. & Berryhill, M. E. (2014), "Real-world objects are more memorable than photographs of objects", *Frontiers in Human Neuroscience*, Vol. 8, p. 837.
- Van Alphen, G. W. H. M. & Graebel, W. P. (1991), "Elasticity of tissues involved in accommodation", *Vision Research*, Vol. 31 No. 7, pp. 1417-1438.
- Ventura, A. C. S., Böhnke, M. & Mojon, D. S. (2001), "Central corneal thickness measurements in patients with normal tension glaucoma, primary open angle glaucoma, pseudoexfoliation glaucoma, or ocular hypertension", *British journal of ophthalmology*, Vol. 85 No. 7, pp. 792-795.
- Waran, V., Narayanan, V., Karuppiah, R., Owen, S. L. & Aziz, T. (2014), "Utility of multimaterial 3D printers in creating models with pathological entities to enhance the training experience of neurosurgeons", *J Neurosurg*, Vol. 120 No. 2, pp. 489-92.
- Wurm, G., Tomancok, B., Pogady, P., Holl, K. & Trenkler, J. (2004), "Cerebrovascular stereolithographic biomodeling for aneurysm surgery", *Journal of Neurosurgery*, Vol. 100 No. 1, pp. 139-145.

- Yap, Y. L., Lai, Y. M., Zhou, H. & Yeong, W. Y. "Compressive strength of thin-walled cellular core by inkjet-based additive manufacturing", in Chua, C. K., Yeong, W. Y., Tan, M. J. & Liu, E.,(Eds.), *Proceedings of 1st International Conference on Progress in Additive Manufacturing in Singapore, 2014*, Research Publishing Services, Singapore, pp. 333-338.
- Yap, Y. L. & Yeong, W. Y. (2014), "Additive manufacture of fashion and jewellery products: a mini review", *Virtual and Physical Prototyping*, Vol. 9 No. 3, pp. 195-201.
- Yap, Y. L. & Yeong, W. Y. (2015), "Shape recovery effect of 3D printed polymeric honeycomb", *Virtual and Physical Prototyping*, Vol. 10 No. 2, pp. 91-99.
- Yeong, W. Y., Chua, C. K., Leong, K. F. & Chandrasekaran, M. (2004), "Rapid prototyping in tissue engineering: challenges and potential", *Trends Biotechnol*, Vol. 22 No. 12, pp. 643-52.
- Yeong, W. Y., Chua, C. K., Leong, K. F., Chandrasekaran, M. & Lee, M.-W. (2005), "Development of scaffolds for tissue engineering using a 3D inkjet model maker", *Virtual modelling and rapid manufacturing-advanced research in virtual and rapid prototyping*, pp. 115-118.
- Yusoff, W. a. Y. W., Ali, H. H. M. & Shukri, M. a. H. M. "Fabrication of surgical cranioplasty biomodel using fused deposition modeling", 2012, pp. 550-554.
- Zardawi, F. M. M. (2013), *Characterisation of Implant Supported Soft Tissue Protheses Produced with 3D Colour Printing Technology*, University of Sheffield.
- Zein, N. N., Hanouneh, I. A., Bishop, P. D., Samaan, M., Eghtesad, B., Quintini, C., Miller, C., Yerian, L. & Klatt, R. (2013), "Three-dimensional print of a liver for preoperative planning in living donor liver transplantation", *Liver Transplantation*, Vol. 19 No. 12, pp. 1304-1310.
- Ziebarth, N. M., Arrieta, E., Feuer, W. J., Moy, V. T., Manns, F. & Parel, J.-M. (2011), "Primate lens capsule elasticity assessed using Atomic Force Microscopy", *Experimental Eye Research*, Vol. 92 No. 6, pp. 490-494.